Inhibition of thrombin activity by a covalent-binding aptamer and reversal by the complementary strand antidote

doi: 10.1039/D0CC08109D

ChemComm
Chemical Communications

Accepted Manuscript

This article can be cited before page numbers have been issued, to do this please use: Y. Tabuchi, J. Yang and M. Taki, *Chem. Commun.*, 2021, DOI: 10.1039/D0CC08109D.

ROYAL SOCIETY OF CHEMISTRY

rsc.li/chemcomm

View Article Online
DOI: 10.1039/D0CC08109D

COMMUNICATION

Inhibition of thrombin activity by a covalent-binding aptamer and reversal by the complementary strand antidote

Yudai Tabuchi, [a, b] Jay Yang[b]* and Masumi Taki [a]*

Received 00th January 20xx,
Accepted 00th January 20xx

DOI: 10.1039/x0xx00000x

Alleviating the potential risk for irreversible adverse drug effects has been an important and challenging issue for the development of covalent drugs. Here we created a DNA-aptamer-type covalent drug by introducing a sulfonyl fluoride warhead at appropriate positions of the thrombin binding aptamer to create the weaponized covalent drugs. We showed a de-activation of thrombin by the novel modality, followed by its re-activation by the complementary strand antidote at an arbitrary time. We envision that such on-demand reversal of covalent drugs alleviates the major concern of potentially irreversible ADEs and accelerate the translational application of covalent aptamer drugs.

Targeted covalent drugs can form permanent bonds to target proteins and, in theory, eternally exert the drug effect.[1-7] This prolonged duration of drug action would reduce the required dosing frequency and improve quality-of-life for patients.[6, 8] However, because of the potential risk for irreversible adverse drug effects (ADEs), a cautious approach towards the covalent drug development has prevailed.[6, 8-10] Many small molecule-, peptide-, and protein-type covalent drugs have been developed.[8, 11-14] In particular, notable progress has been made in utilizing the sulfur fluoride exchange (SuFEx) click chemistry and protein engineering to create novel covalently binding proteins with superior performance compared to the non-covalent counterpart.[14, 15] However, to the best of our knowledge, none have overcome the potential risk of irreversible ADEs.

Nucleic acid aptamers (i.e., single-stranded small oligonucleotides) are emerging as an attractive class of drugs.[16-20] Aptamers have been shown to exhibit high binding affinity and selectivity[21] with dissociation constants typically in the nM and even pM ranges when properly selected against a target.[22, 23] Since the target affinity arises from the correct folding of the single-stranded aptamer, the addition of complementary strand (CS) oligonucleotide as an antidote results in the formation of a double-strand (DS), and release of the aptamer drug from the target.[19] Kinetics of the DS formation are rapid and effective *in vivo*, and the reversal of an anticoagulant aptamer has been demonstrated.[18, 24]

Here we report the creation of an aptamer-type covalent drug that covalently binds to thrombin, inhibiting its enzymatic activity while retaining on-demand reversal by a CS antidote. We start with the well-characterized thrombin binding aptamer (TBA) which is a 15-base DNA oligonucleotide identified by SELEX (Systematic Evolution of Ligands by EXponential enrichment).[23, 25-27] TBA inhibits thrombin enzymatic activity resulting in the prolongation of clotting time, *in vitro*[28, 29], and effective anticoagulation, *in vivo*.[30] A warhead (i.e., sulfonyl fluoride[31, 32]) with a relatively long spacer was introduced at appropriate positions of TBA to create the weaponized covalent drugs. The linker was placed outside the presumed TBA-thrombin interaction interface to minimize potential interference with the binding of TBA to thrombin. The reactive warhead placed at the end of the extended linker maximized the chances of covalent bond formation at sites away from the enzyme catalytic active site and the TBA binding site. Upon addition of the CS antidote, TBA was dislodged from thrombin, reversing the anticoagulant effect while still covalently bound to the target protein (Fig. 1).

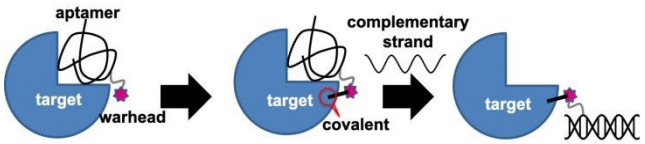

Fig. 1 Summary of a covalent-binding aptamer. A warhead (red star) conjugated aptamer (folded string) binds to its target protein (blue) (left). A covalent-bond is formed between the warhead-conjugated aptamer and the target protein (middle), resulting in semi-permanent drug action. Introduction of the CS antidote removes the aptamer from the binding site and reverses the permanent drug action (right).

To create the covalent-binding TBA, we introduced an azidated (i.e., N_3-) warhead to an alkyne-containing TBA by the

[a] *Department of Engineering Science, Bioscience and Technology Program, The Graduate School of Informatics and Engineering, The University of Electro-Communications (UEC), 1-5-1 Chofugaoka, Chofu, Tokyo 182-8585, Japan.*
[b] *Department of Anesthesiology, University of Wisconsin, School of Medicine and Public Health, Madison, Wisconsin 53706 United States, and Department of GI Surgery II, Hokkaido Univ Grad Sch Medicine, Sapporo, Hokkaido, Japan.*
E-mail: taki@pc.uec.ac.jp; Tel: +81-42-443-5980 (M.T.)
E-mail: jyang75@wisc.edu; Tel: +81-70-1391-0185 (J.Y.)
Electronic Supplementary Information (ESI) available: [details of any supplementary information available should be included here]. See DOI: 10.1039/x0xx00000x

copper(I)-catalyzed azide-alkyne cycloaddition (CuAAC) reaction[33]. As the warhead, we chose an aryl-sulfonyl fluoride (Ar-SO_2F) derivative to maximize the potential of covalent-binding with the target protein without lack of protein-specificity; it spontaneously forms a covalent bond with a proximal nucleophilic amino acid (i.e., serine, threonine, lysine, tyrosine, cysteine, or histidine) via a reaction.[31, 32, 34, 35] As identified in Fig. S2, N_3-Ar-SO_2F was synthesized (Fig. 2a), and it was introduced on designated thymine residues (T_x) to obtain TBA isomers (TBA_X) (Fig. 2b). TBA_3 and TBA_{12}, in which the warhead is attached to T_3 and T_{12}, respectively, facing the TBA-thrombin interaction interface, were designed on the basis of the known crystal structure[36] (Fig. S3). TBA_9 was also created in which T_9 modified by the warhead faced the side opposite from the interaction interface. The purity of each warhead-conjugated TBA was determined to be about 95% by liquid chromatography (Fig. S4). Invariant circular dichroism spectra (Fig. S5) showed that introducing the warhead did not grossly alter the TBA folded structure.

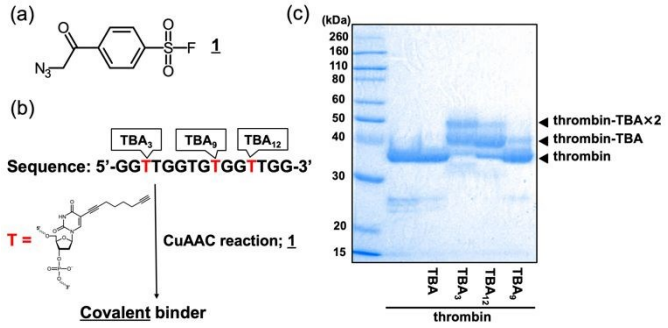

Fig. 2 Identification of covalent-binding TBA. (a) Chemical structure of the azidated warhead. (b) Creation of the warhead conjugated TBA. Azidated warhead was introduced to an appropriate position of TBA; an alkyne-containing thymine whose position is highlighted in red was conjugated with the azidated warhead by CuAAC reaction. (c) Covalent-binding between each warhead-conjugated TBA and thrombin, confirmed by 13% SDS-PAGE, followed by CBB staining. Each black arrow represents the band of the thrombin and thrombin-TBA conjugate, respectively.

Next, we evaluated the covalent-binding ability of each warhead-conjugated TBA. TBA_3 and TBA_{12}, incubated with thrombin, induced persistent mobility shift of the protein on gel electrophoresis where the protein bands were visualized by Coomassie Brilliant Blue (CBB) staining. This suggests that a stable covalent bond was formed between the respective modified aptamers and thrombin. In contrast, native TBA (i.e., negative control possessing no warhead) and TBA_9 did not induce significant mobility shift (Fig. 2c). The warhead location-dependent covalent-binding with thrombin also strongly suggests that the SuFEx reaction is target-specific and not due to a non-specific interaction of warhead. For further experiments, we exclusively used TBA_3 because the covalent-binding efficiency was the highest among them. The covalent-binding efficiency was improved by increasing the molar concentrations of TBA_3 against a fixed thrombin amount. At higher molar concentrations of TBA_3, two separated bands were seen (Fig. 3a). Of note, the competition assay with native TBA demonstrated a decrease in both two separated bands (Fig. S6), suggesting that the TBA_3-mono-adduct and bis-adduct form covalent-bond formation at two distinct thrombin residues while sharing the same binding site with native TBA (i.e., exosite I[36]). We believe the TBA_3 tethered to thrombin exhibits a finite off rate from exosite I, allowing entry of a second TBA_3 that covalently binds to a different residue in thrombin, resulting in the bis-adduct. The covalent-binding efficiency increased with time up to 90% within 60-120 minutes. The final covalent-binding efficiency of TBA_3 to thrombin proceeded to 90% in time- and concentration-dependent manners (Fig. 3b, c).

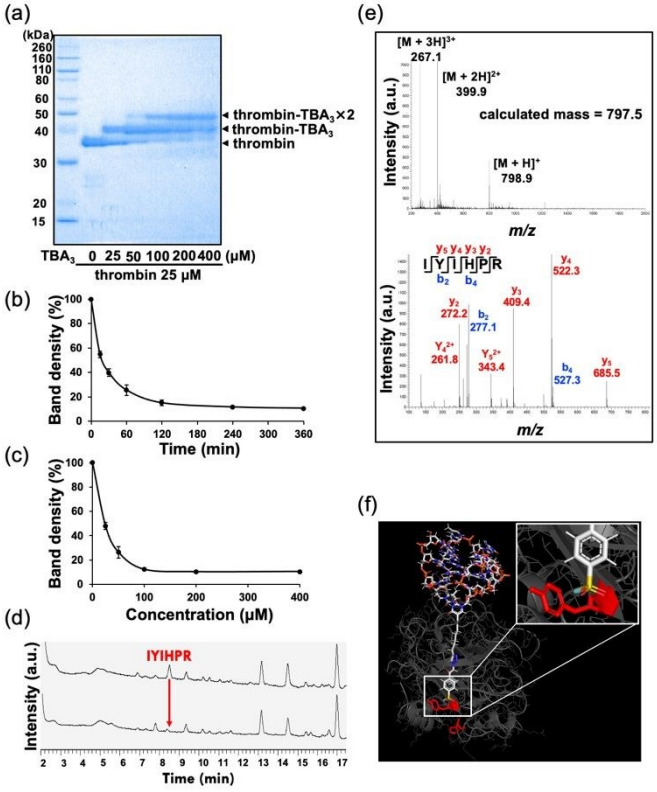

Fig. 3 Covalent-binding ability of TBA_3. (a) Concentration-dependent mobility shift of thrombin on gel, confirmed by 13% SDS-PAGE followed by CBB staining. (b) Time-dependent change of covalent-binding efficiency. The density of the unreacted-thrombin band at 0 minute was normalized to 100%, and the relative density of each incubation time was quantified. (c) Concentration-dependent change of covalent-binding efficiency. The density of the unreacted-thrombin band in the absence of TBA_3 was normalized to 100%, and the relative density of each concentration of TBA_3 was quantified. (d) LC profile of trypsinized fragments of thrombin without (top) or with (bottom) TBA_3. A single fragment peak of thrombin, identified as IYIHPR by MS and MS/MS, diminished after the covalent binding of TBA_3. (e) MS and MS/MS spectra of the reduced peak. (f) Molecular docking simulation of the TBA_3 (shown as a stick) to thrombin (PDB ID: 1HAO) using cosgene of myPresto. Fluorine atom in the warhead (cyan) and a folded ribbon cartoon thrombin (grey) with the putative TBA_3 covalently bound residues Y88 and H91 (red).

The potential of TBA_3 covalent-binding site was explored by trypsinization of the covalently bound molecule followed by liquid chromatography-tandem mass spectrometry (LC-MS/MS). Because of the technical difficulty of identifying a peptide-oligonucleotide complex by the MS analysis[37] (see the supporting information section), we monitored the disappearance of a specific peak among the trypsinized

fragments of thrombin on the LC profile. A significant decrease in a peptide fragment corresponding to IYIHPR sequence was observed only when TBA_3 was present (Fig. 3d, e), indicating that the location of the putative TBA_3 covalent-binding site is within this peptide span and outside of the thrombin enzyme catalytic site (Fig. 3f).

Thrombin activity inhibition by TBA_3 was monitored by a time-dependent change of optical density at 288 nm (i.e., turbidimetric assay), which corresponds to thrombin-induced fibrin aggregation.[38] The activity decreased in a concentration-dependent manner with an IC50 of 3.5 ± 0.1 nM for native TBA (Fig. 4a, b), whereas TBA_3 showed a 3-fold greater potency with an IC50 of 1.2 ± 0.1 nM (N=3, P = 0.00048) (Fig. 4c, d). It is plausible that the tethered TBA_3 covalently bound to thrombin increased the effective local concentration[39], allowing the desired thrombin inhibition to be achieved at a lower bulk concentration. An automated coagulometer monitored change in the thrombin-dependent clotting time, and as expected, the mean clotting times in the presence of TBA_3 at 5 nM and 1 nM were significantly increased compared to native TBA (Table 1).

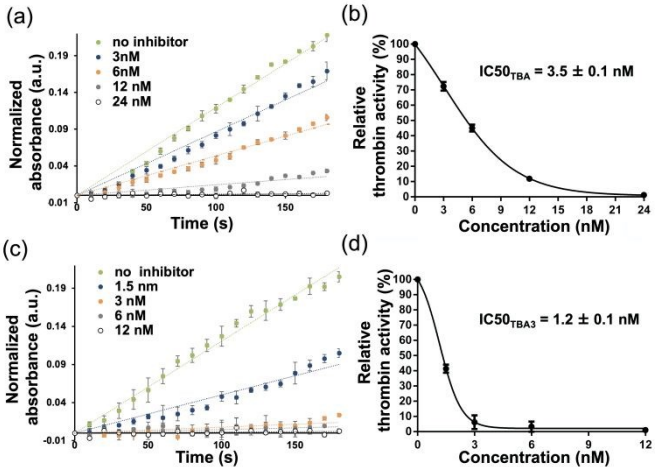

Fig. 4 Comparison of thrombin inhibition activity between native TBA and TBA_3 by turbidimetric assay. (a) Time-dependent thrombin inhibition by native TBA with different concentration. The maximum absorbance (288 nm) of fibrin polymerization at 0 second was normalized to 0% and plotted against time. The plot was fit by a line, and the slope value was quantified as a thrombin activity. (b) The thrombin activity in the absence of inhibitor was normalized to 100%, and the relative thrombin activity of each concentration was quantified. (c) and (d) were performed as above but using TBA_3.

Finally, the on-demand reversal property of TBA_3 was confirmed by the following experiments. A carboxyfluorescein (FAM)-tagged CS incubated with TBA_3 covalently bound thrombin resulted in a fluorescent signal at the expected molecular mass consistent with the FAM-CS forming a double strand with the thrombin bound-TBA (Fig. 5a). Fluorescent bands did not appear in the presence of serum proteins, indicating high specificity of TBA_3 toward thrombin (Fig. 5b). Turbidimetric thrombin enzymatic assay confirmed a CS antidote concentration-dependent reactivation of thrombin with an EC50 of 2.3 ± 0.2 nM for native TBA (Fig. 5c, d), and an EC50 of 4.6 nM ± 0.3 for TBA_3 (Fig. 5e, f). The difference in CS antidote EC50 was statistically significant (N = 3, P = 0.015) by a paired t-test. As expected, the clotting times increased by native TBA or TBA_3 were entirely normalized by the CS antidote (Table 1).

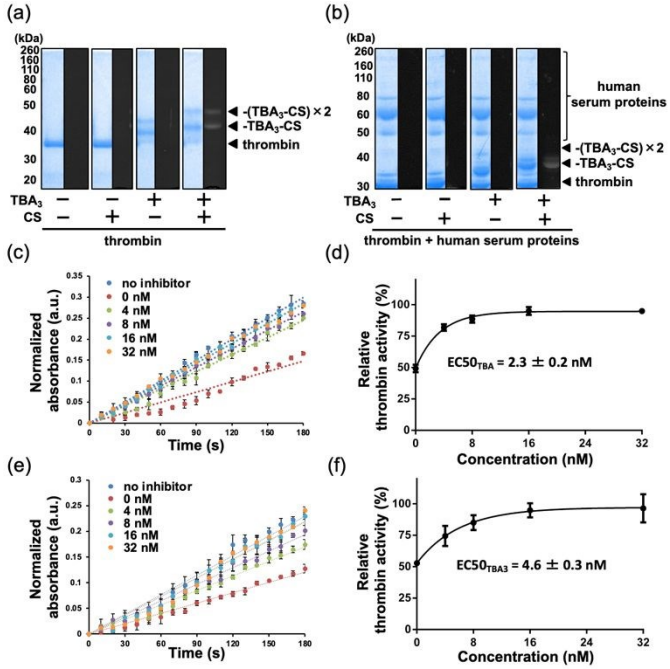

Fig. 5 On-demand reversal property of TBA_3 by CS antidote. (a) TBA-specific duplex formation of CS antidote confirmed by 13% SDS-PAGE/fluorescence imaging. Whole proteins were visualized by CBB staining (left panel of each lane), and a complex of TBA_3 covalently bound for thrombin and FAM-CS was visualized by fluorescence in the same gel (right panel of each lane). (b) Specific covalent binding between TBA_3 and thrombin, confirmed by the same procedure as in (a) except in the presence of human serum (40%). (c) The reversal of thrombin inhibition activity of native TBA confirmed by the turbidimetric assay with increasing concentrations of CS antidote. All runs contained IC50 concentration of native TBA, which resulted in approximately 50% thrombin activity in the absence of CS antidote. The maximum absorbance (288 nm) of fibrin polymerization at 0 seconds was normalized to 0% and plotted against time. The plot was fit by a line and the slope quantified as thrombin activity. (d) The thrombin activity in the absence of inhibitor was normalized to 100%, and relative thrombin activity at each concentration of CS antidote was quantified. (e) and (f) were performed as in (c) and (d) but by using TBA_3.

In conclusion, we created a covalent-binding DNA aptamer that targets thrombin by introducing a sulfonyl fluoride warhead into appropriate positions of the TBA. The covalent-binding TBA demonstrated high-affinity inhibition of the thrombin activity and showed on-demand reversal property of this drug action by the CS antidote. While we did not examine the *in vivo* pharmacokinetic of TBA_3, prolonged inhibition of the target protein is expected by extension of pharmacological half-life mediated by the covalent binding, regardless of the macroscopically observable pharmacokinetic half-life. Accordingly, covalent-binding aptamers would enable *in vivo* use of aptamer drugs as a covalent drug by circumventing the pharmacokinetic and drug action duration limitations while maintaining the desirable features such as on-demand reversal property, high affinity, target selectivity, easy production, and lack of immunogenic response.[40, 41] Furthermore, weaponizing aptamers with SuFEx-warhead is likely applicable in developing

covalent aptamers targeting a wide range of target proteins as a general method. We believe that these advantages will mitigate the major concern of covalent drugs and accelerate the translation to human usage.

Table 1. Prolongation of clotting time by native TBA and TBA_3.

Sample	Concentration[a]	CS antidote	Clotting time (s)[b]	P value[c]
No inhibitor	-	-	21 ± 1	0
native TBA	1 nM	-	26 ± 2	0.0065
TBA_3	1 nM	-	41 ± 3	0.00016
native TBA	5 nM	-	40 ± 3	-
TBA_3	5 nM	-	200 ~	-
TBA_3	1 nM	5 nM	21 ± 1	0.80
TBA_3	1 nM	20 nM	20 ± 1	0.86
TBA_3	5 nM	5 nM	39 ± 1	0.0080
TBA_3	5 nM	20 nM	22 ± 2	0.19

[a]Native TBA or TBA_3 was incubated with thrombin for 3 hours at 37°C and fibrinogen solution added to give a final concentration of 13 nM thrombin, 2 mg/mL fibrinogen, and native TBA or TBA_3 varied as shown. [b]Clotting times were measured using an automated coagulometer. [c]Values are mean ± S.E.M. from six independent experiments. All groups were compared with the group of no inhibitor by a paired t-test. $P < 0.05$ was considered to be statistically significant.

This work was supported by a JSPS KAKENHI grant (#20J22890) to Y. T. We thank Drs. Y. Ge and Y. Lee (U Wisconsin) for the use of their experimental facilities.

Notes and references

1. T. A. Baillie, *Angew. Chem. Int. Ed. Engl.*, 2016, **55**, 13408-13421.
2. J. Gan, H. Zhang and W. G. Humphreys, *Chem. Res. Toxicol.*, 2016, **29**, 2040-2057.
3. A. J. Smith, X. Zhang, A. G. Leach and K. N. Houk, *J. Med. Chem.*, 2009, **52**, 225-233.
4. D. S. Johnson, E. Weerapana and B. F. Cravatt, *Future Med. Chem.*, 2010, **2**, 949-964.
5. R. Lagoutte, R. Patouret and N. Winssinger, *Curr. Opin. Chem. Biol.*, 2017, **39**, 54-63.
6. J. Singh, R. C. Petter, T. A. Baillie and A. Whitty, *Nat. Rev. Drug Discov.*, 2011, **10**, 307-317.
7. R. A. Copeland, D. L. Pompliano and T. D. Meek, *Nat. Rev. Drug Discov.*, 2006, **5**, 730-739.
8. R. A. Bauer, *Drug Discov Today*, 2015, **20**, 1061-1073.
9. W. J. Pichler, D. J. Naisbitt and B. K. Park, *J. Allergy Clin. Immunol.*, 2011, **127**, S74-81.
10. Y. O. Yang, Y. Z. Shu and W. G. Humphreys, *Chem. Res. Toxicol.*, 2016, **29**, 109-116.
11. T. Zhang, J. M. Hatcher, M. Teng, N. S. Gray and M. Kostic, *Cell Chem. Biol.*, 2019, **26**, 1486-1500.
12. L. Gambini, C. Baggio, P. Udompholkul, J. Jossart, A. F. Salem, J. J. P. Perry and M. Pellecchia, *J. Med. Chem.*, 2019, **62**, 5616-5627.
13. Q. Li, Q. Chen, P. C. Klauser, M. Li, F. Zheng, N. Wang, X. Li, Q. Zhang, X. Fu, Q. Wang, Y. Xu and L. Wang, *Cell*, 2020, **182**, 85-97 e16.
14. V. Y. Berdan, P. C. Klauser and L. Wang, *Bioorg. Med. Chem.*, 2020, **29**, 115896.
15. Q. Zheng, J. L. Woehl, S. Kitamura, D. Santos-Martins, C. J. Smedley, G. Li, S. Forli, J. E. Moses, D. W. Wolan and K. B. Sharpless, *Proc. Natl. Acad. Sci. U S A*, 2019, **116**, 18808-18814.
16. K. Wakui, T. Yoshitomi, A. Yamaguchi, M. Tsuchida, S. Saito, M. Shibukawa, H. Furusho and K. Yoshimoto, *Mol. Ther. Nucleic Acids*, 2019, **16**, 348-359.
17. C. P. Rusconi, E. Scardino, J. Layzer, G. A. Pitoc, T. L. Ortel, D. Monroe and B. A. Sullenger, *Nature*, 2002, **419**, 90-94.
18. H. Stoll, H. Steinle, N. Wilhelm, L. Hann, S. J. Kunnakattu, M. Narita, C. Schlensak, H. P. Wendel and M. Avci-Adali, *Molecules*, 2017, **22**, 954-967.
19. K. M. Bompiani, R. S. Woodruff, R. C. Becker, S. M. Nimjee and B. A. Sullenger, *Curr. Pharm. Biotechnol.*, 2012, **13**, 1924-1934.
20. T. Adachi and Y. Nakamura, *Molecules*, 2019, **24**, 4229-4243.
21. X. Chen, L. Qiu, R. Cai, C. Cui, L. Li, J. H. Jiang and W. Tan, *ACS Appl. Mater. Interfaces.*, 2020, **12**, 37845-37850.
22. Y. Zhang, B. S. Lai and M. Juhas, *Molecules*, 2019, **24**, 941-963.
23. J. Zhou and J. Rossi, *Nat. Rev. Drug. Discov.*, 2017, **16**, 181-202.
24. C. P. Rusconi, J. D. Roberts, G. A. Pitoc, S. M. Nimjee, R. R. White, G. Quick, Jr., E. Scardino, W. P. Fay and B. A. Sullenger, *Nat. Biotechnol.*, 2004, **22**, 1423-1428.
25. A. D. Ellington and J. W. Szostak, *Nature*, 1990, **346**, 818-822.
26. L. C. Bock, L. C. Griffin, J. A. Latham, E. H. Vermaas and J. J. Toole, *Nature*, 1992, **355**, 564-566.
27. M. Blind and M. Blank, *Mol Ther Nucleic Acids*, 2015, **4**, e223.
28. L. C. Bock, L. C. Griffin, J. A. Latham, E. H. Vermaas and J. J. Toole, *Nature*, 1992, **355**, 564-566.
29. W. X. Li, A. V. Kaplan, G. W. Grant, J. J. Toole and L. L. Leung, *Blood*, 1994, **83**, 677-682.
30. L. C. Griffin, G. F. Tidmarsh, L. C. Bock, J. J. Toole and L. L. Leung, *Blood*, 1993, **81**, 3271-3276.
31. A. Narayanan and L. H. Jones, *Chem. Sci.*, 2015, **6**, 2650-2659.
32. H. Mukherjee, J. Debreczeni, J. Breed, S. Tentarelli, B. Aquila, J. E. Dowling, A. Whitty and N. P. Grimster, *Org. Biomol. Chem.*, 2017, **15**, 9685-9695.
33. V. V. Rostovtsev, L. G. Green, V. V. Fokin and K. B. Sharpless, *Angew. Chem. Int. Ed. Engl.*, 2002, **41**, 2596-2599.
34. J. Dong, L. Krasnova, M. G. Finn and K. B. Sharpless, *Angew. Chem. Int. Ed. Engl.*, 2014, **53**, 9430-9448.
35. A. S. Barrow, C. J. Smedley, Q. Zheng, S. Li, J. Dong and J. E. Moses, *Chem. Soc. Rev.*, 2019, **48**, 4731-4758.
36. I. Russo Krauss, A. Merlino, A. Randazzo, E. Novellino, L. Mazzarella and F. Sica, *Nucleic Acids Res.*, 2012, **40**, 8119-8128.
37. I. G. Gut, W. A. Jeffery, D. J. C. Pappin and S. Beck, *Rapid. Commun. Mass Sp.*, 1997, **11**, 43-50.
38. E. G. Zavyalova, A. D. Protopopova, I. V. Yaminsky and A. M. Kopylov, *Anal. Biochem.*, 2012, **421**, 234-239.
39. R. Hansen, U. Peters, A. Babbar, Y. Chen, J. Feng, M. R. Janes, L. S. Li, P. Ren, Y. Liu and P. P. Zarrinkar, *Nat. Struct. Mol. Biol.*, 2018, **25**, 454-462.
40. G. Eyetech Study, *Ophthalmology*, 2003, **110**, 979-986.
41. G. Eyetech Study, *Retina*, 2002, **22**, 143-152.